Reaction Rate Prediction in the Supercritical Region of $H^{\cdot} + OH^{-} \rightarrow e_{aq}^{-} + H_2O$ using μSR

Tait Du[1], Guangdong Liu [2], John Beninger [3], Khashayar Ghandi[4]
[1] Mount Allison University, New Brunswick, Canada
(tdu@mta.ca)
[2] (gliu@mta.ca)
[3] (jgbeninger@mta.ca)
[4] (kghandi@mta.ca)

An Undergraduate Level Submission

Summary

Knowledge of reaction rates in the supercritical region for reactions caused by the radiolysis of water is needed to prevent damage to future Supercritical Water-Cooled reactors. In particular, the $H^{\cdot} + OH^{-} \rightarrow e_{aq}^{-} + H_2O$ reaction is examined experimentally within the supercritical region by usage of muon spin rotation spectroscopy. Using the obtained data and the "cage effect" theory, the reaction was modelled and plateau-like behaviour near the critical point was accounted for.

1. Introduction

Power generation is the cornerstone of modern civilization, requiring increasingly sophisticated means to supply growing demand. Nuclear fission remains one of the powerful tools at our disposal, with development of Generation IV reactors. This next generation of reactors is not only expected to be more efficient in terms of power production, but also expected to have increased safety capabilities [1].

Out of the six proposed designs for Gen IV reactors, the Super-Critical Water-Cooled reactor (SCWR) design is of particular interest to Canadian researchers. When water is put under supercritical conditions which are characterised by temperature of or exceeding 374 ºC and pressure of or exceeding 22.1Mpa for light water, it no longer undergoes liquid-steam transitions and remains a single-phase system with properties similar to both the liquid and steam phases [2]. Therefore, in contrast to traditional LWC reactors that require steam/water separators and recirculation loops, only a once-through cycle is necessary for the operation of the SCWR because the coolant is fed directly into the turbines. This significantly simplifies the reactor design, lowering required construction capital. Furthermore, the higher temperature differentials involved in a SCWR allows for a thermal efficiency of 44% which is better than the 34%-36% found in normal reactors and a SCWR coolant leak would have less environmental impact compared to proposed Sodium-Cooled Fast reactors [1].

One barrier hindering the implementation of the SCWR design, is the lack of knowledge on effects of radiation in the SCW. When exposed to ionizing radiation, water can produce various reactive intermediates, [3] that could generate species that would be damaging to the reactor core. It is therefore pertinent that the reaction kinetics of the various reactions caused by the radiolysis of supercritical

water be understood so that negative effects can be minimized. This paper presents research on the reaction $H^{\cdot} + OH^{-} \rightarrow e_{aq}^{-} + H_2O$. Few studies reach or pass the critical point which makes it difficult to model behaviour in the supercritical region [3]. Elliot and Bartels have collected data up to 350 Cº for this reaction [4][5][6][7] however to our knowledge no group had collected data past the critical point. Using μSR, our group has reached past the critical point, up to approximately 425 Cº.

2. Methodology

2.1 Transverse Field Muon Spin Rotation (TF-μSR)

Muons, the positive μ^+ in this case, are elementary particles with a mean lifetime of 2.2μs that decay into a positron and neutrino-antineutrino pair. For the purposes of our research, μ^+ is treated as light proton with one-ninth proton mass. When μ^+ encounters an electron it can combine to form Muonium (Mu), which is nearly identical to the hydrogen atom in terms of Bohr radius and ionization potential: This can allow Mu to be treated as an isotope of hydrogen. Furthermore, muons can easily penetrate through solid materials, removing the need for optical access to the sample being examined which is needed for pulse radiolysis [8].

When groups of muons are generated from the weak interaction decay of pions, they are nearly 100% spin polarized: This spin polarization mostly extends to the positron decay product. When a beam of muons is fired into a sample, the muons quickly combine with electrons to form Mu, this can be used to probe reactions involving hydrogen atoms. The application of a magnetic field transverse to muon spin causes the muon to precess at a frequency characteristic of their environment [9]. When Mu decays, it fires off a positron at an angle that is determined by the angle of its spin relative to a defined axis. This property allows the muon environment to be probed through muon decay. To accomplish this, muons are first sent through a detector which starts an electronic clock as shown in Fig.1. The muons promptly combine with electrons to form Mu which reacts with other compounds as a short-lived hydrogen. The time taken for the decay positron to hit a detector perpendicular to the muon detector is dependent on the angle of Mu decay as shown in Fig.1 [10]. The decay rate can be used to determine the rate constant of the desired reaction if the concentration of the other reactant is known.

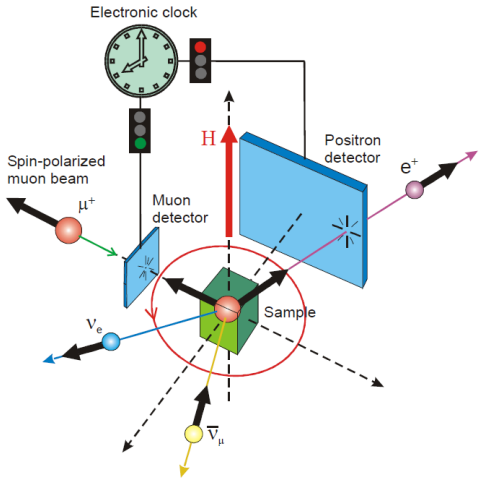

Fig.1 Schematic of TF-μSR setup [10]

2.2 High Pressure and Temperature Setup

In order to do measurements at the supercritical region, the sample has to be heated and pressurized to the critical point. This is accomplished using the design in Fig.2.

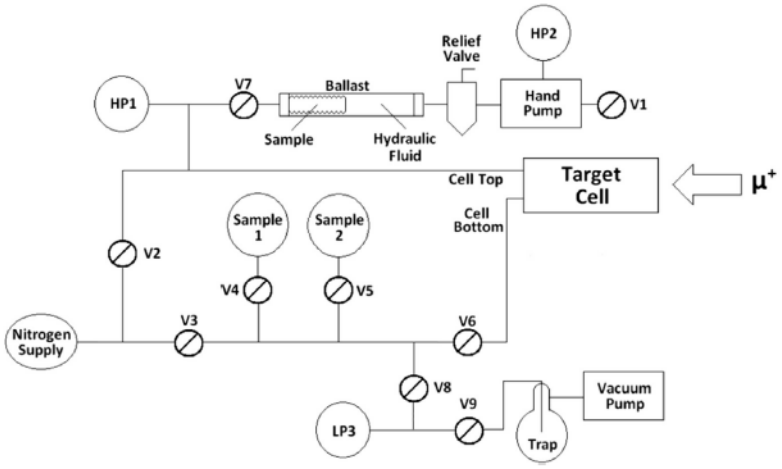

Fig.2 Design of high pressure/temperature setup. V*n* represents high pressure valves while HP*n* and LP*n* represent high and low pressure sensors respectively. [9] (see text for description).

The apparatus is flushed multiple times with the nitrogen to remove oxygen from the system after pumping with a vacuum pump. The sample being used is then moved into the target cell made of a titanium alloy [9]. Since no optical window is needed, the target cell can be brought past 350 Cº [8]. The apparatus separates the pressurization and the heating implements for the cell into two components. Two conducting coils moving in opposite directions and then an insulator surround the target cell. This allows the sample to be heated by running a current through the wire, but the magnetic field caused by the current is minimized due to the configuration of the wire. The pressure can be independently increased by using the hydraulic pump. Separating the heating and pressurization methods allows for control of pressure and temperature independently.

3. Results and Discussion

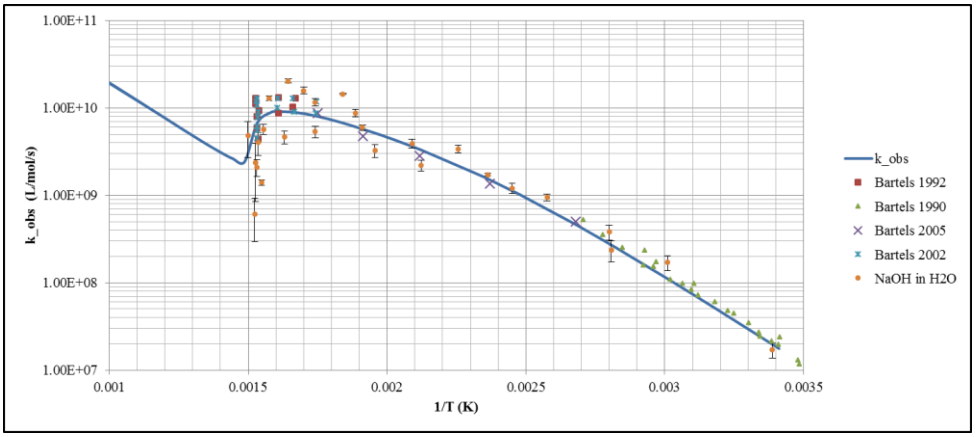

Fig.3 Experimental Data and Modeled Observed Rate Constant of Reaction [3][4][5][6][7]

A ($dm^3\ mol^{-1}\ s^{-1}$)	E_a (kJ mol^{-1})	$p_R k_{gas}$ ($dm^3 mol^{-1} s^{-1}$)	$B(r)$ ($dm^3 Pa\ mol^{-1}\ K^{-1}$)	Pressure (bar)
1.59E+14	39.0	2.12E+18	2.43E+05	250

Table.1 Fitting Parameters

The observed rate constant k_{obs} in Fig.3 is controlled by two rate constants in Noyes equation:

$$\frac{1}{k_{obs}} = \frac{1}{k_{diff}} + \frac{1}{k_{react}} \quad (1)$$

In this equation, k_{diff} is the diffusion rate constant, which measures how fast reactants can approach each other. On the other hand, k_{react} is the chemical reaction rate constant [11]. Usually k_{diff} is calculated using the Stokes-Einstein equation (SEE), is proportional to temperature and is inversely proportional to solvent viscosity. Our method of calculation is not different from SEE, however we combine all constants into one constant B(r), so k_{diff} becomes:

$$k_{diff} = B(r) \times \frac{T}{\eta} \quad (2)$$

Where T is temperature, and η is viscosity. Normally k_{react} has an Arrhenius temperature dependence, but our calculations include an additional factor fr to account for the cage effect [11]:

$$k_{react} = f_R\, A e^{\frac{-Ea}{RT}} \quad (3)$$

In the above equation, A is the pre-exponential factor, Ea is the activation energy, and R is the gas constant. The efficiency factor of collisions per encounter, f_R, has the form:

$$f_R = \frac{P_R k_{gas} \times \left(\frac{\eta}{T}\right)}{k_{diff} + P_R k_{gas} \times \left(\frac{\eta}{T}\right)} \quad (4)$$

Where, $p_R k_{gas}$ is the rate of potentially reactive collisions and k_{diff} is the rate of encounters. Our value for $p_R k_{gas}$ is proportional to solvent viscosity, is inversely proportional to the temperature, and is therefore multiplied by $\left(\frac{\eta}{T}\right)$ [11]. The pre-exponential factor A, activation energy Ea, rate of potentially reactive collisions $p_R k_{gas}$ and the constant $B(r)$ are assumed to be temperature independent fitting parameters in this work, and are used in fitting experimental data.

Overall our modeled k_{obs} fits the experimental data gathered by Bartels' group. In Bartels' 2005 paper, they suggested that there should be two separate Arrhenius regions, 33.1 kJ mol^{-1} for below 100 °C, and 22.1 kJ mol^{-1} for above. Bartels and co-workers address a few assumptions that might explain the reasoning: multiple reaction steps, quantum tunneling and semi-classical transition state. Using our model, we managed to fit the multiple ranges using a single activation energy. That being said, our model does not fully account for the drop in k_{obs} near the critical point. In the future, we plan on modifying our model to factor in critical fluctuations in order to describe k_{obs} near the critical point with better relation with experimental data. In addition, we also plan on using multiple activation parameters for our model to better relate with Bartels' suggestion of the existence of multiple Arrhenius regions.

4. Conclusions

Using the μSR method we obtained results which are similar to previously published data in the 20-350 C° range and data showing a large drop in reaction rate in the region surrounding the critical point. The

observed drop of the reaction rate around the critical point is partially explained using the cage effect theory, but our model does not decrease as much as the experimental data does. For future consideration we will consider modeling in the critical fluctuations of density in supercritical fluids as well as using multiple activation parameters depending on the temperature range of the fit.

5. References

[1] Generation IV International Forum, "Technology roadmap update for generation IV nuclear energy systems.", January 2014
[2] P.L. Kirillov, "Supercritical water cooled reactors", *Thermal Engineering*, 2008, vol. 55, no. 5, pp. 361–364
[3] A. Elliot, and D.M. Bartels, "The reaction set, rate constants and g-values for the simulation of the radiolysis of light water over the range 20 to 350 C based on information available in 2008." *Atomic Energy of Canada, Ltd.*, 2009
[4] J. Cline, K. Takahashi, , T.W. Marin, C.D. Jonah, and D. M. Bartels, "Pulse Radiolysis of Supercritical Water. 1. Reactions between Hydrophobic and Anionic Species" *J. Phys. Chem. A*, vol.106, no.51, 2002, pp.12260–12269
[5] P. Han and D. M. Bartels, "Hydrogen/deuterium isotope effects in water radiolysis. 4. The mechanism of aquated hydrogen atom ≒ solvated electron interconversion," *J. Phys. Chem.*, vol. 96, no. 12, 1992, pp. 4899–4906.
[6] T. W. Marin, C. D. Jonah, and D. M. Bartels, "Reaction of hydrogen atoms with hydroxide ions in high-temperature and high-pressure water.," *J. Phys. Chem. A*, vol. 109, no. 9, 2005, pp. 1843–1848.
[7] P. Han, and D. M. Bartels, "Reevaluation of Arrhenius parameters for hydrogen atom + hydroxide → (e-)aq + water and the enthalpy and entropy of hydrated electrons," *J. Phys. Chem.*, vol. 94, no. 18, 1990, pp. 7294–7299.
[8] K. Ghandi, A. MacLean, **"**Muons as hyperfine interaction probes in chemistry", *Hyperfine Interactions*, vol. 230, no. 1-3, 2015, pp. 230, 17-34
[9] C.D. Alcorn, J-C Brodovitch, P.W. Percival, M. Smith, K. Ghandi, "Kinetics of the reaction between H and superheated water probed with muonium", *Chemical Physics*, vol.435, 2014, Pages 29-39
[10] TRIUMF. Centre for Molecular & Materials Science. http://musr.ca/intro/musr/ muSRBrochure.pdf (accessed Feb. 9th, 2014)
[11] K. Ghandi et al., "Near-diffusion-controlled reactions of muonium in sub- and supercritical water", *Physical Chemistry Chemical Physics*, no.4, 2002, pp.586-595